Research Article

Nanomedicine

Modulating cellular autophagy for controlled antiretroviral drug release

Midhun B Thomas[‡,1], Divya Prakash Gnanadhas[‡,1], Prasanta K Dash[1], Jatin Machhi[1], Zhiyi Lin[1], JoEllyn McMillan[1], Benson Edagwa[1], Harris Gelbard[2], Howard E Gendelman[1] & Santhi Gorantla*[,1]

[1]Department of Pharmacology & Experimental Neuroscience, University of Nebraska Medical Centre, Omaha, NE 68198, USA

[2]Department of Neurology, University of Rochester Medical Centre, Rochester, NY 14618, USA

*Author for correspondence: Tel.:+1 402 559 8910; Fax:+ 402 550 3744; sgorantla@unmc.edu

[‡]Authors contributed equally

Aim: Pharmacologic agents that affect autophagy were tested for their abilities to enhance macrophage nanoformulated antiretroviral drug (ARV) depots and its slow release. **Methods:** These agents included URMC-099, rapamycin, metformin, desmethylclomipramine, 2-hydroxy-β-cyclodextrin (HBC) and clonidine. Each was administered with nanoformulated atazanavir (ATV) nanoparticles to human monocyte-derived macrophages. ARV retention, antiretroviral activity and nanocrystal autophagosomal formation were evaluated. **Results:** URMC-099, HBC and clonidine retained ATV. HBC, URMC-099 and rapamycin improved intracellular ATV retention. URMC-099 proved superior among the group in affecting antiretroviral activities. **Conclusion:** Autophagy inducing agents, notably URMC-099, facilitate nanoformulated ARV depots and lead to sustained release and improved antiretroviral responses. As such, they may be considered for development as part of long acting antiretroviral treatment regimens.

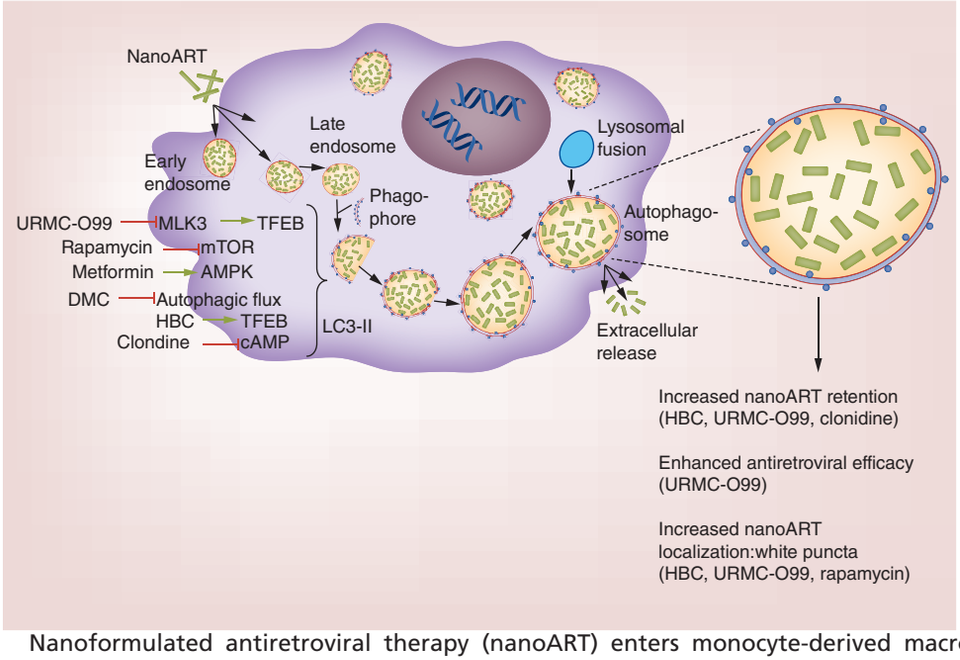

Nanoformulated antiretroviral therapy (nanoART) enters monocyte-derived macrophages through clathrin-coated pits and are then transported into the cell's early and late endosomes. After treatment with inducers of autophagy, the phagophore sequesters an area of cytoplasm to form double membraned autophagosomes. Lipid conjugation leads to the formation of LC3II associated autophagic vesicles. The late endosome fuses with autophagosomes transferring the nanoART cargo, which in turn fuses with lysosomes leading to the degradation of accumulated cargo. However, if terminal stages are blocked these processes can lead to the accumulation of drug cargos and a slower drug degradation. How, and to what extent,

Future Medicine

autophagy inducers influence the cell's drug depots is not yet well understood, but likely reflects multiple intracellular mechanisms. URMC-099, a mixed lineage kinase inhibitor, induces autophagy through nuclear translocation of the transcription factor EB. Rapamycin forms complex with FKB12 that specifically acts as an allosteric inhibitor of the mammalian target of rapamycin to speed autophagy. Metformin causes inhibition of the mitochondrial chain complex 1 that in turn indirectly activates AMP-activated protein kinase becoming a negative regulator of mammalian target of rapamycin. Desmethylclomipramine induces autophagy through its abilities to interfere with the autophagic flux by blocking the degradation of the cytoplasmic cargo. Transcription factor EB regulates autophagy and lysosomal biogenesis by 2-hydroxy-β-cyclodextrin. Clonidine induces autophagy through the activation of the Gi signaling pathway that results in the reduction of cAMP levels caused by the inhibition of adenylyl cyclase. All of these autophagy inducers facilitate autophagosome formation that leads to the retention of nanoART in the autophagosome. This ensures the sustained extracellular release of antiretroviral drugs for a prolonged period of time and enhances antiretroviral activities.

First draft submitted: 29 June 2018; Accepted for publication: 27 July 2018; Published online: 21 August 2018

Keywords: 2-hydroxy-β-cyclodextrin (HBC) • autophagy • clonidine • desmethylclomipramine (DMC) • long acting slow effective release antiretroviral therapy • metformin • monocyte-derived macrophages • rapamycin • URMC-099

Despite remarkable success of antiretroviral therapy (ART) in the treatment of HIV-1 infections challenges still remain. These include the requirements for lifelong treatment, strict patient regimen adherence, drug toxicities, viral resistance and inherent failures to eliminate infections [1,2]. The recent development of long acting antiretroviral drug (ARV) nanoformulations provides new opportunities for overcoming these limitations and offers added therapeutic benefits to infected patients. These include, but are not limited to, improved therapeutic outcomes seen by extending the drugs' apparent half-life, optimizing drug penetrance into viral reservoirs and reducing viral mutation rates [3–6]. Based on our own laboratory's recent successes in developing long-acting ART [7–14], we have aggressively pursued strategies aimed at establishing long-lived intracellular drug depots. To realize such goals, our research focused on the enhancement of cell-based depots that could further increase ARV endosomal storage, affect drug delivery and release, and directly restrict ongoing infections at sites of viral growth. These would occur, in tandem, during optimization of immune-based antiretroviral innate responses associated with migratory, phagocytic and secretory monocyte–macrophage activities [15–18]. If long-lived ARV depots are established they would facilitate controlled drug release and aid in ART induced reduction of viral loads and HIV-1 transmission [5,6].

For the generation of long-acting nanoARV, our laboratories employ poloxamer surfactants [15,19–21]. Several nanocarriers were developed in recent years that affect intracellular-controlled drug release. Mesoporous silica nanoparticles are used as a controlled release drug delivery system for intracellular protein and nucleic acids [22,23]. Such biomaterials are commonly used for agent encapsulation due to inherent biocompatibility, large surface area and tunable pore sizes. Polymer based suspensions have also been evaluated in the delivery of antiretrovirals and other water insoluble compounds. Sustained release of rilpivirine (RPV) was observed from nanosuspensions stabilized by polyethylene–polypropylene glycol (poloxamer 338) and PEGylated tocopheryl succinate ester [24]. Dou *et al.*, have shown that nanosuspensions of indinavir stabilized by Lipoid E80 elicit sustained release of drug for up to 14 days [25]. Liposomes conjugated with mannose and galactose have been used for the encapsulation of stavudine facilitating targeted delivery [26]. Dendrimer nanocarriers can deliver efavirenz to human monocytes and macrophages, while peptide nanocarriers facilitate intracellular drug delivery [27,28].

We have used macrophages as carriers of nanoARVs with an intent to deliver drugs to HIV-1 tissue reservoirs [10,14,15,29]. Based on the specific known cellular functions of macrophages, the cells' high cytoplasmic to nuclear ratios and their inherent rapid mobility, macrophages serve as the target cell for the ARV nanoparticles. Macrophages phagocytose nanoparticulated ARVs forming drug depots. These are contained within endosomal compartments and as such extend the apparent half-life of the drugs being tested [9,30,31]. We recently found that autophagy serves to facilitate this process further by sequestering the drug depots into autophagosomes. URMC-099 served as an ARV depot booster and its control on autophagy, inflammation, drug metabolism and excretion [7,9,29]. To further investigate URMC-099's effects on long acting ARVs depot formulation, a comparative analysis of autophagy inducers was performed. These agents included URMC-099, rapamycin – a mTORC1 inhibitor, clonidine – a mTOR independent imidazoline-1 receptor agonist, 2-hydroxy-β-cyclodextrin (HBC) – a

transcription factor EB mediator (TFEB), metformin – an 5′ AMP-activated protein kinase (AMPK) activator and mTOR inhibitor and desmethylclomipramine (DMC) – an agent that interferes with autophagic flux by affecting autophagosome-lysosome blockades. HIV-1 infected human monocyte-derived macrophages (MDM) treated with nanoformulated atazanavir (nanoATV) and autophagy agents showed significantly increased ATV retention and viral suppression with URMC-099 demonstrating the optimal activities. These data highlight the broad abilities of autophagy inducers to affect long-lived depots of ARVs and as such serve to increase the drug's half-life and activity.

Materials & methods

Isolation & cultivation of human monocyte–macrophages

Human MDMs were used to determine drug depot formation and antiretroviral efficacy of nanoATV. Human monocytes were isolated by centrifugal elutriation from leukopaks obtained from HIV-1/2 and hepatitis seronegative donors. Monocytes were cultured in DMEM medium supplemented with 10% heat inactivated human serum, 2 mM L-glutamine, 50 μg/ml gentamicin, 10 μg/ml ciprofloxacin and 1000 U/ml recombinant human macrophage-colony stimulating factor. Macrophage-colony stimulating factor was prepared from culture fluids of 5/9m alpha3-18 cells (ATCC®, CRL-10154™). Cells were maintained at 37°C in a 5% CO_2 incubator. Media were half exchanged every 2 days. Monocytes differentiate into macrophages like cells after 7 days in culture [32].

Autophagy inducers & cell vitality measures

URMC-099 (MW: 421.54 g/mol) was synthesized by Califia Bio, Inc. (CA, USA). Rapamycin, clonidine, HBC, metformin and DMC were obtained from Sigma-Aldrich (MO, USA). Cell vitality was evaluated by measuring mitochondrial dehydrogenase activity in MDM using the 3-(4,5-dimethylthiazol-2-yl)-2,5-diphenyltriazolium bromide (MTT) assay. Varying concentrations of autophagy agents were added to the MDM cultures. The concentrations used were URMC-O99 (0.1, 0.5, 1.0 and 2.0 μM), rapamycin (1, 10, 20 and 40 nM), clonidine (0.01, 0.1, 1 and 10 μM), HBC (0.001, 0.01, 0.1 and 1 mM), metformin (0.01, 0.05, 0.1 and 0.5 mM) and DMC (0.01, 0.05, 0.1 and 0.5 μM). On days 3, 7, 10 and 14; the media were removed, and the cells were incubated with MTT (5 mg/ml) for 30 min at 37°C. Mitochondrial dehydrogenase reduced MTT to insoluble formazan crystals which were subsequently solubilized by DMSO; the absorbance was measured at 570 nm (SynergyMX, multimode spectrophotometer, BioTek, VT, USA).

Creation of nanoATV

NanoATV was prepared by high-pressure homogenization (Avestin EmulsiFlex-C3; Avestin, Inc., Ottawa, ON, Canada) as described previously [15,29]. For preparation of nanoATV, free-base ATV (1% w/v) and poloxamer P407 (0.2%, w/v) was suspended in a solution of P407 (0.2% w/v) in 10 mM HEPES, pH 7.8 for 16 h and homogenized at 20,000 psi until the desired particle size and polydispersity index (PdI) were achieved. CF633 labelled nanoATV was prepared by homogenizing a suspension of free-base ATV (1% w/v) in a solution mixture of P407 (0.4%, w/v) and CF633-P407 (0.1%, w/v) in 10 mM HEPES, pH 7.8. Effective diameter, PdI and ζ potential were measured by dynamic light scattering (Malvern Zetasizer Nano Series Nano-ZS, Malvern Instruments, MA, USA). Drug loading was determined by HPLC with UV/Vis detection. ATV was quantitated by comparison of peak areas with those of known standards (0.05–50 μg/ml in methanol) [29]. ATV-sulfate was purchased from Gyma Laboratories of America, Inc., (NY, USA) and transformed into free base using triethylamine. P407 was purchased from Sigma-Aldrich. CF633-succinimidyl ester (CF633) was purchased from Biotium (CA, USA).

Western blot assays

On days 3, 7, 10 and 14, MDM incubated with each of the autophagy inducers were lysed (CellLytic, Sigma-Aldrich) in the presence of protease and phosphatase inhibitors (Thermo Fisher Scientific, MA, USA). After incubation at room temperature for 10 min, the cell lysates were centrifuged at 12,000 rpm for 10 min and the supernatant was collected. Protein concentrations were determined in the supernatant using Micro BCA Protein Assay Kit (Thermo Fisher Scientific). The proteins were separated on a 12% SDS-polyacrylamide gel (Bio-Rad, CA, USA) by electrophoresis (100 V for 90 min). Separated proteins were transferred onto an activated Polyvinylidene difluoride (PVDF) membrane over 1 h at 70 V. The membrane was then blocked with 5% bovine serum albumin in Tris-buffered saline with 0.05% Tween-20 at room temperature for 1 h. Subsequently, the membrane was incubated overnight at 4°C with antibodies that included LC3B (NB100, Novus Biologicals, MN, USA), β-actin (A2228, Sigma-Aldrich), beclin 1 (BECN1) (H300, Santa Cruz Biotechnology, TX, USA) and SQSTM1/P62 (PM045,

MBL International, MA, USA). After washing the membrane 3× with Tris-buffered saline and Tween-20, it was incubated with HRP-conjugated secondary antibodies (Santa Cruz Biotechnology) for 1 h at room temperature. The protein bands were detected as chemiluminescent signals and analyzed with a myECL imager (Thermo Fisher Scientific).

Measure of nanoATV retention & extracellular release

MDM were incubated with 100 μM nanoATV for 16 h then washed 3× with phosphate-buffered saline (PBS). This was followed by the addition of fresh media supplemented with autophagy inducers at the following concentrations: URMC-O99 (1 μM), rapamycin (10 nM), clonidine (0.5 μM), HBC (20 μM), metformin (0.5 mM) and DMC (0.5 μM). MDM were further cultured for up to 14 days. On days 3, 7, 10, and 14 following nanoATV treatments, media were collected for the measurement of extracellularly released ATV; the cells were collected by scrapping and centrifuged at 8000 rpm for 10 min. Cell pellets were stored at -80°C for drug measurements. For ATV quantifications, the cell pellet was suspended in 200 μl of HPLC-grade methanol, probe sonicated for 5 s, and then centrifuged for 10 min at 8000 rpm. Each sample was analyzed in triplicates. ATV in each sample was quantified by the comparison of peak area to the standard curve of ATV (0.025–100 μg/ml) in methanol as described [33].

The media collected on the specified day were vortexed for 10 s with 1 ml of HPLC grade methanol being added to 150 μl of media. The samples were subsequently placed at -20°C for 30 min, after which they were centrifuged at 14,000 rpm and 4°C for 10 min. The supernatants were transferred to new Eppendorf tubes and placed in speed-vac to generate dried pellets. The pellets were resuspended in 75 μl of HPLC grade methanol and vortexed for 10 s. The samples were sonicated in water bath for 5 min and centrifuged at 14,000 rpm and 4°C for 10 min. 75 μl of each sample supernatant was transferred to a 96-well plate and drug released from the nanoATV quantified by the HPLC.

Confocal microscopy

MDM were cultured in a 24-well glass bottom plate and pretreated with 50 μM CF633-labeled nanoATV for 16 h. Cells were then washed 3× with PBS and incubated with each of the autophagy inducers. On the 12th day of treatment, MDM were transfected with Premo Autophagy Sensor LC3B-GFP (Thermo Fisher Scientific). After 48 h, cells were washed and fixed with 4% paraformaldehyde. The cells were stained with 4′,6-diamidino-2-phenylindole (DAPI) and a cover slip placed over it using Prolong Gold Anti-fade Reagent (Invitrogen, OR, USA). The images were taken with the LSM 710 Zeiss Confocal Laser Scanning Microscope and analyzed with Zen 2 (blue edition).

HIV-1 infection & drug treatments

MDM were infected with HIV-1_{ADA} at a multiplicity of infection of 0.01. After 4 h of infection, cells were washed with PBS and fresh medium was added. MDM were treated with nanoATV either before or after HIV-1 infection. Excluding the measures of drug retention, a subtherapeutic concentration of the nanoATV (1 μM) was employed to test the viral suppressive effects of the autophagy inducers. MDM were treated with nanoATV at various time points from 1 day before to 3 days after infection. The duration of treatment was 12 h and afterward the cells were washed and replaced with medium containing each of the autophagy inducers.

Measurements of HIV-1 infection

To determine the antiretroviral activity of nanoformulations, the cell medium was collected for measurement of HIV-1 reverse transcriptase (RT) activity. 10 μl of the culture supernatants from the infected cells were added to 10 μl reaction mixture containing 100 mM Tris-HCl (pH 7.9), 300 mM KCl, 10 mM DTT and 0.1% nonylphenoxylpolyethoxyl-ethanol-40 in a 96-well plate and incubated at 37°C for 15 min. This was followed by the addition of 25 μl of a solution containing 50 mM Tris-HCl (pH 7.9), 150 mM KCl, 5 mM DTT, 15 mM $MgCl_2$, 0.05% nonylphenoxylpolyethoxyl-ethanol-40, 10 μg/ml poly(A), 0.250 U/ml oligo d(T) and 10 μCi/ml ^{3}H-TTP to each well. After 18 h incubation at 37°C, 50 μl of ice-cold 10% trichloroacetic acid was added to each well and the contents were harvested onto glass fiber filters and assessed for ^{3}H-TTP incorporation by β-scintillation spectroscopy [34].

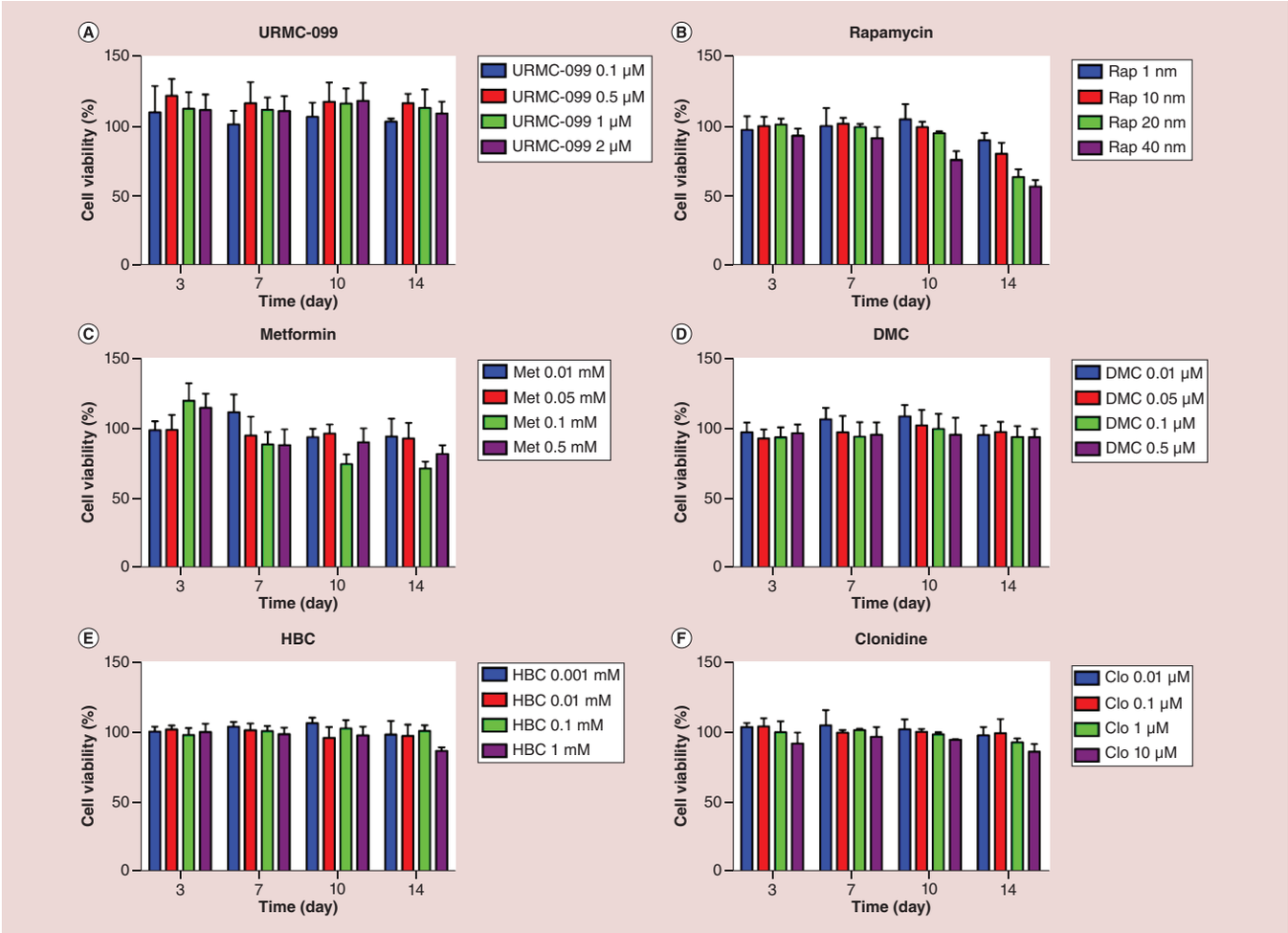

Figure 1. Cell mitochondrial vitality. MDM following treatment with **(A)** URMC-099, **(B)** rapamycin, **(C)** metformin, **(D)** DMC, **(E)** HBC and **(F)** clonidine at various concentrations were analyzed by the MTT assay. MDMs were incubated with MTT (5 mg/ml) for 30 min at 37°C. Depending on viability, MTT was reduced to insoluble formazan crystals which was solubilized into a purple colored solution by DMSO. Results are shown as percentage of cell viability as compared with untreated MDM. Data are represented as mean ± SD for n = 4 samples/group.
DMC: Desmethylclomipramine; HBC: 2-hydroxy-β-cyclodextrin; MDM: Monocyte-derived macrophage; MTT: (3-(4,5-dimethylthiazol-2-yl)-2,5-diphenyltriazolium bromide; SD: Standard deviation.

Statistical analyses

Data were analyzed using GraphPad Prism 6.0 software (GraphPad Software) and Microsoft Excel. Two-way factorial ANOVA and multiple comparisons using Tukey and Bonferroni's *post hoc* tests were performed for the studies on HIV infection over time in MDM. Significant differences were determined at a p-value of less than 0.05.

Results

Expression of autophagy markers in macrophages

Firstly, in order to select the optimal concentration of the autophagy inducers for studies, four concentrations of each inducer were tested for up to 14 days for macrophage vitality. On days 3, 7, 10 and 14, MTT tests were performed on the drug-treated MDM (Figure 1). Based on the cell vitality measures, noncytotoxic concentrations of each of the autophagy inducer was employed for the experiments. The autophagy drugs tested were URMC-099 (1 μM), rapamycin (10 nM), clonidine (0.5 μM), HBC (20 μM), metformin (0.5 mM) and DMC (0.5 μM). To confirm the induction of autophagy, linked cellular pathways were examined by western blot tests. These included BECN1, microtubule-associated protein 1 light chain 3 β (LC3BI/LC3BII) and p62 (Figure 2A). The most prominent induction observed was with URMC-099 (Figure 2B–D). On days 10 and 14, a significant increase in p62 and

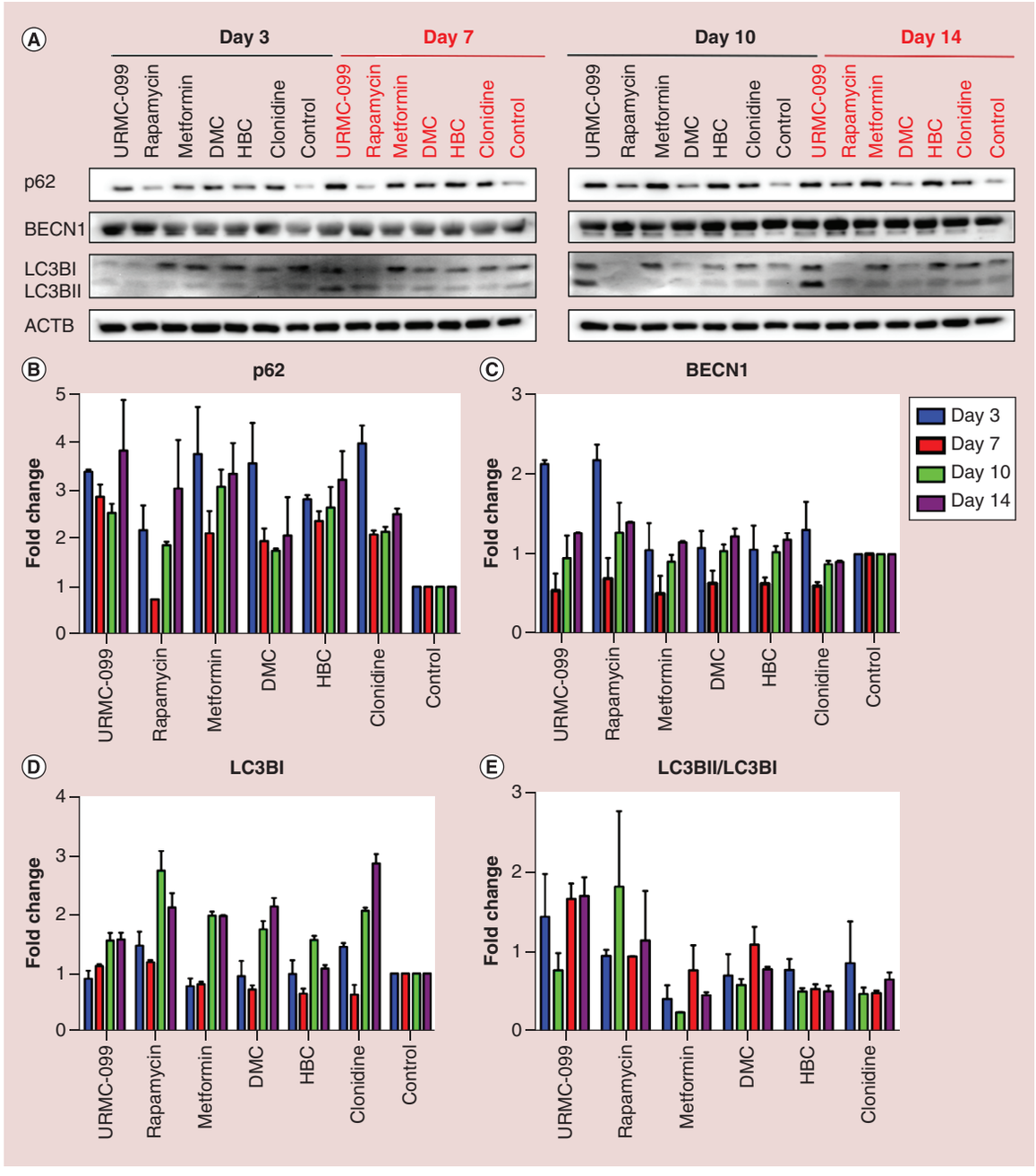

Figure 2. Analyses of induced autophagy markers. Human MDMs were incubated with the panel of autophagy inducers tested independently for 14 days after which the samples were analyzed by western blot tests **(A)**. The effect of each inducer on p62 **(B)**, BECN1 **(C)**, LC3BI **(D)** and LC3BII/I **(E)** was performed by quantification of the protein bands normalized to ACTB using ImageJ2 software (n = 3).
ACTB: β-actin; BECN1: Beclin 1; DMC: Desmethylclomipramine; HBC: 2-hydroxy-β-cyclodextrin; LC3BI/II: Light chain 3 β; MDM: Monocyte-derived macrophage.

BECN1 was observed and the LC3BII/LC3BI ratio was greater than 1. These data demonstrated that autophagy was induced but autophagosome lysosome fusion was not complete and autophagy flux was reduced. Autophagosomes accumulated with URMC-099 treatment were previously shown to be the reservoirs of nanoformulated ARVs [23]. Increases in p62 reflected partial fusion of the autophagosome-lysosome with peak activities at days 10 and 14.

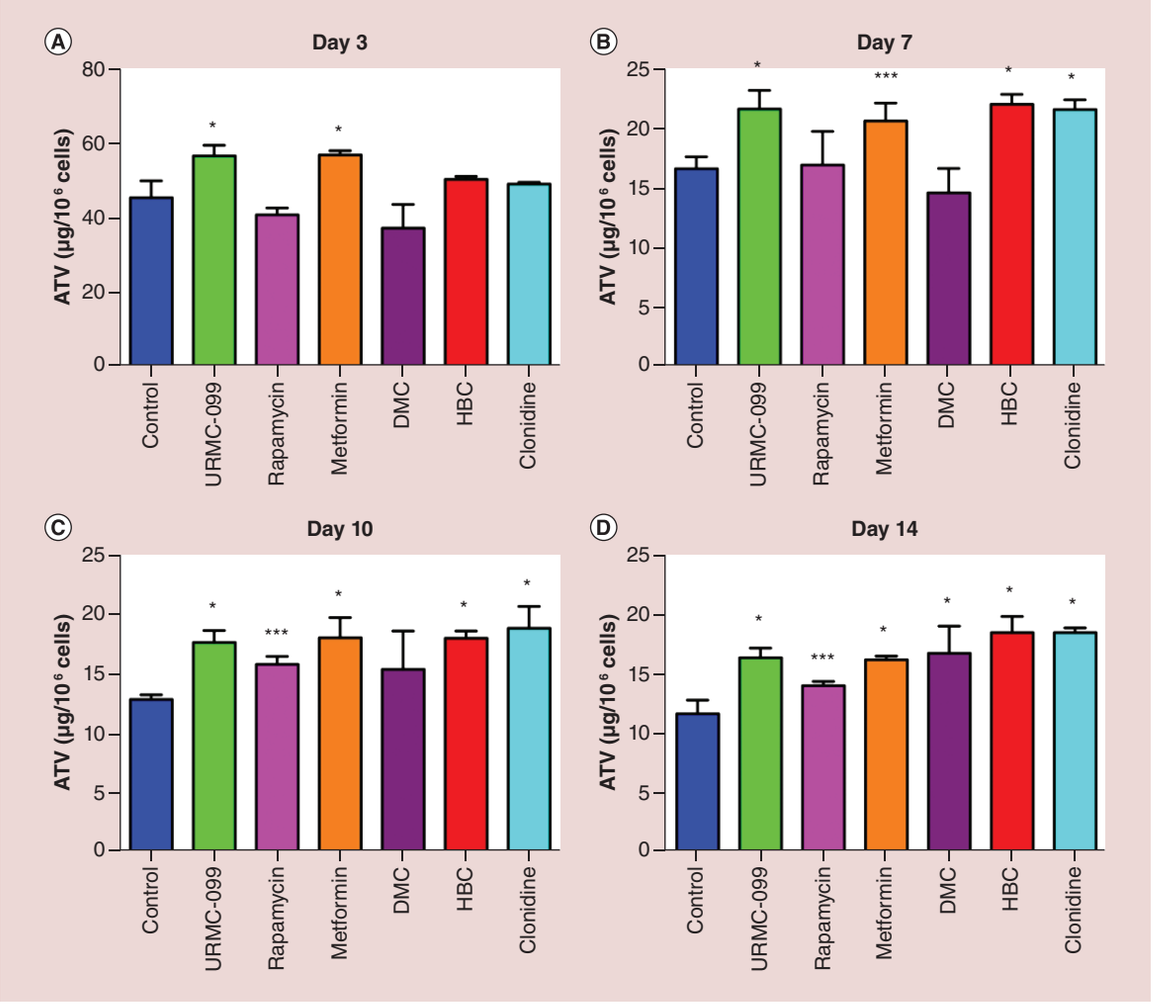

Figure 3. Macrophage drug retention. This was determined after MDMs were treated with nanoATV for 16 h with the panel of autophagy inducers for 14 days. After each scheduled time point, cells were harvested and pelleted. The intracellular drug concentrations were analyzed by HPLC on days 3, 7, 10 and 14 **(A–D)**. Comparisons between the control and each of the autophagy inducers was performed by Tukey's multiple comparison ANOVA test. Data are represented as mean ± SD for n = 6 samples per group. *$p < 0.0001$, **$p < 0.001$ and ***$p < 0.01$.
ATV: Atazanavir; MDM: Monocyte-derived macrophage; SD: Standard deviation.

Autophagy & nanoformulated ATV retention

To study the role of autophagy inducers in nanoATV retention in MDM, the cells were treated with 100 µM nanoATV for 14 days. The nanoATV formulations were 327.4 ± 2.08 nm in size and demonstrated a PdI of 0.18 ± 0.01 and a ζ potential of -8.08 ± 0.64 mV. Drug concentrations were assessed with and without the autophagy inducers at days 3, 7, 10 and 14. On day 3, untreated (control i.e., not treated with autophagy inducers) cells retained 45 µg of nanoATV/10^6 cells. URMC-099 and metformin treated cells retained 57 µg of nanoATV/10^6 cells with a $p < 0.0001$ compared with the control (Figure 3A). The amount was reduced to 16 µg of nanoATV/10^6 in untreated cells at day 7, while URMC-099, metformin, HBC and clonidine treated cells showed 22 µg of nanoATV/10^6 cells (Figure 3B). An ATV concentration of approximately 17 µg of nanoATV/10^6 cells was obtained for HBC, metformin, URMC-099 and clonidine compared with 12 µg at day 10 for untreated cells (Figure 3C). Drug levels were found to be increased by 1.4-fold on treatment with the above mentioned autophagy inducers compared with the untreated cells. The drug levels were sustained for most autophagy inducers through day 14 (Figure 3D). Except for rapamycin, all the other autophagy inducers showed a statistical significant difference of $p < 0.0001$ with the control on day 14. Each of the autophagy inducers were compared with the control at each time point by the Tukey's multiple comparison test. All autophagy inducers tested demonstrated increases

in retained ATV compared with controls. These data are in agreement with the extracellular release pattern of nanoATV and indirectly proportional to drug retention levels. Hence, HBC, clonidine and URMC-099 facilitates slow sustained release of nanoATV (Supplementary Figure 1).

NanoATV localization in autophagosomes

We next tested intracellular localization of ATV nanoparticles. MDM were treated with CF633 labelled nanoATV in the presence of each of the autophagy inducers. Cells were transfected with GFP-tagged LC3B and the colocalization with CF633 labelled nanoATV appeared as white puncta (Figure 4). The colocalization studied were performed at day 14 after nanoATV treatments to visualize the differences in drug retention capacities in autophagosomes between different autophagy inducers as optimized in our previous study [35]. Increased fluorescent signals from nanoATV cell depots and LC3B were observed in autophagy drug treated MDM compared with controls. Quantitative measures of the colocalization showed that drug retention in autophagosomes was significantly increased in the presence of autophagy inducers (Figure 5). HBC showed the highest average signal followed by URMC-099 and rapamycin when compared with other autophagy inducers without significant differences among the drugs for autophagosomal drug depot localization. All the autophagy inducers except for metformin had a statistically significant difference with the control ($p < 0.0001$). Similar results were seen for CF633 labelled nanoformulated RPV with the highest signals observed for URMC-099, rapamycin and HBC (Supplementary Figures 2 & 3).

Autophagy inducers facilitate nanoATV antiretroviral activities

We have previously shown that URMC-099 induce autophagy that enhances ATV retention in autophagosomes thereby improving antiretroviral responses of nanoATV [35]. Whether these results could be expanded beyond URMC-099 and involve other autophagy inducers was next tested in the current studies. HIV-1_{ADA} infected MDM were treated with nanoATV at a subtherapeutic concentration (1 μM) with and without the autophagy inducers. Active HIV-1 replication was determined by RT activity in culture supernatants tested at days 3, 6, 9, 12 and 15 after viral infection. When nanoATV was added 1 day before HIV-1 challenge, maximum suppression of viral replication was observed masking any of the effect of autophagy inducers (Figure 6A1–F1). When nanoATV was added 1 day postinfection, URMC-099 (Figure 6A2) and metformin (Figure 6C2) showed up to a twofold decrease in RT activity compared with nanoATV alone. All the autophagy inducers except HBC and DMC had a significant effect on the antiretroviral efficacy when nanoATV was added 3 days after infection. When cells were treated with URMC-099 in combination with nanoATV, a reduction in viral replication by 1.82-fold was observed when compared with nanoATV alone. Similarly, co-administration of other autophagy inducers with nanoATV showed that metformin produced a 1.77-fold reduction, while rapamycin and clonidine produced 1.34- and 1.38-fold reduction, respectively (Figure 6A3–F3). All autophagy inducers, with the exception of HBC, when given in combination with nanoATV to HIV-1 infected MDMs showed a statistically significant difference of $p < 0.0001$ on days 9, 12 and 15 in comparison when the nanoATV was given alone. URMC-O99 provided the highest activity in enhancing nanoATV suppression of the viral infection. Autophagy inducers themselves also affected HIV-1 replication. Both rapamycin and DMC showed antiretroviral activity when given alone as opposed to the other autophagy inducers, as they produced a approximately 1.64-fold in viral replication (Figure 6B & D). However, DMC in combination with nanoATV did not produce a significant suppression in viral replication (Figure 6D1–D3). URMC-099 alone had limited effects on HIV-1 replication [11,35].

Discussion

We report, for the first time, the abilities of autophagy agents to affect antiretroviral activities of a select long acting ARV nanoformulation. To this end when a variety of autophagy inducers and URMC-099 were tested side by side, each were shown to extend ARV nanoparticle retention and antiretroviral activities to differential levels. The administration of nanoATV with each autophagy inducer extended the retention of nanoATV in MDM. Nanoformulated drugs form intracellular drug depots in macrophages by sequestering drug nanocrystals into early, recycling and late endosomes [7,9,11,31,35–40]. When nanoATV was co-administered, most notably, with URMC-099, its retention was increased inside autophagosomes. Enhanced antiretroviral responses were also recorded. The mechanism of these activities were linked to the stimulation of autophagy but halted at the stage of lysosomal degradation of the cargo [11,35]. By controlling the dynamics of particle trafficking inside the cell with autophagy induction, sustained intracellular drug depots and extended half-life of nanoARVs were achieved. Hence, we studied autophagy inducers as possible boosting agents to enhance ART cellular drug depots and slow the rate of

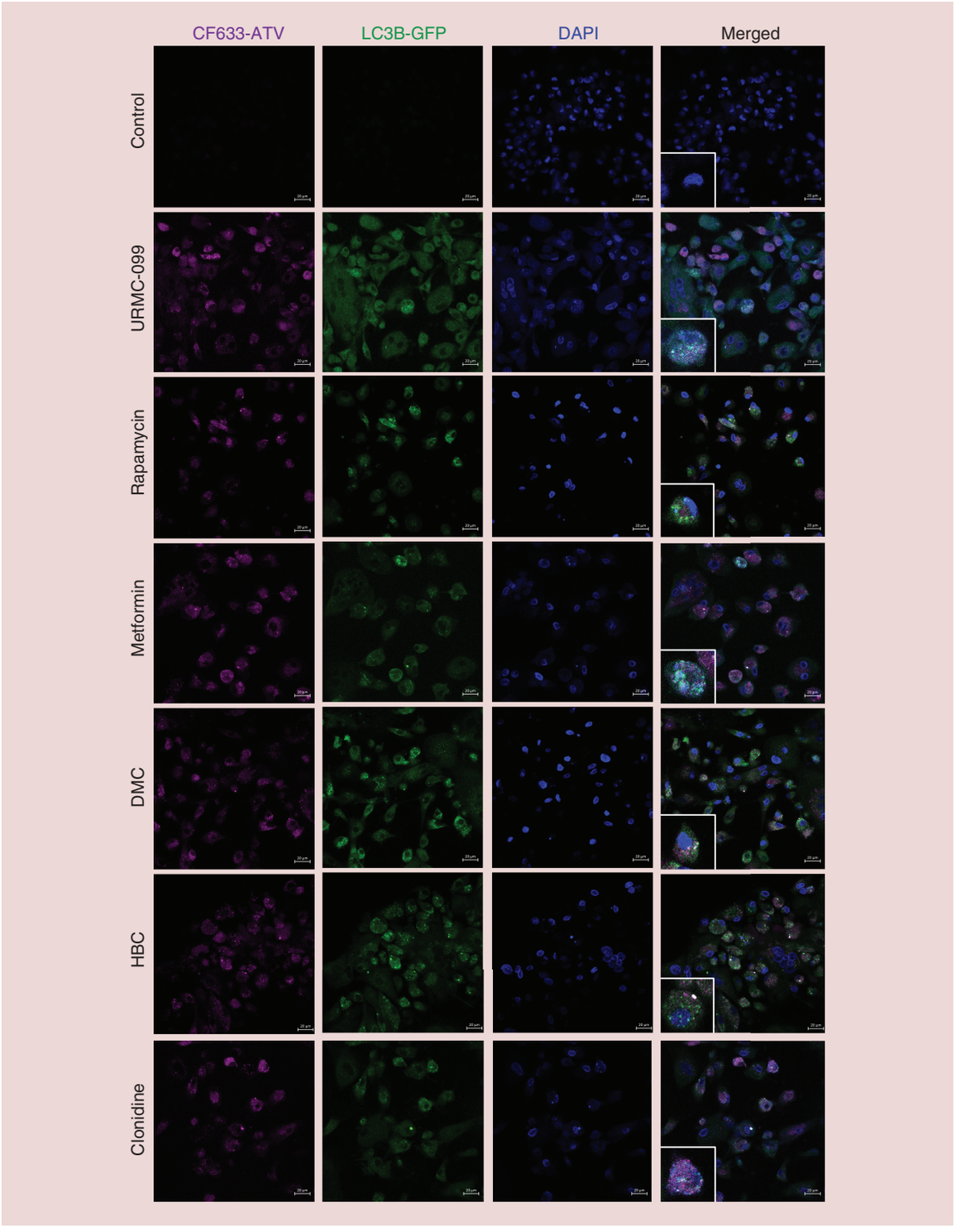

Figure 4. Autophagosomal retention of atazanavir. Human MDM were treated with CF633 labeled nanoATV (red) for 16 h followed by the panel of autophagy inducers for 14 days. Cells were transfected with a LC3B-GFP construct (green), stained with DAPI (blue) and analyzed by confocal microscopy. Scale bar: 20 μm
ATV: Atazanavir; MDM: Monocyte-derived macrophage.

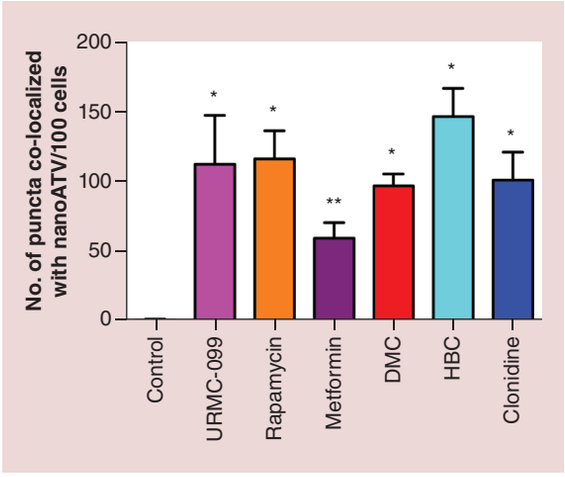

Figure 5. Quantitative measurement of white puncta by light chain 3 ß antiretroviral colocalization. Multiple comparisons between control and the means of each sample was done using the Tukey's multiple comparison ANOVA test. Data are represented as mean ± SD for n = 5 per group. *$p < 0.0001$ and **$p < 0.001$.
SD: Standard deviation.

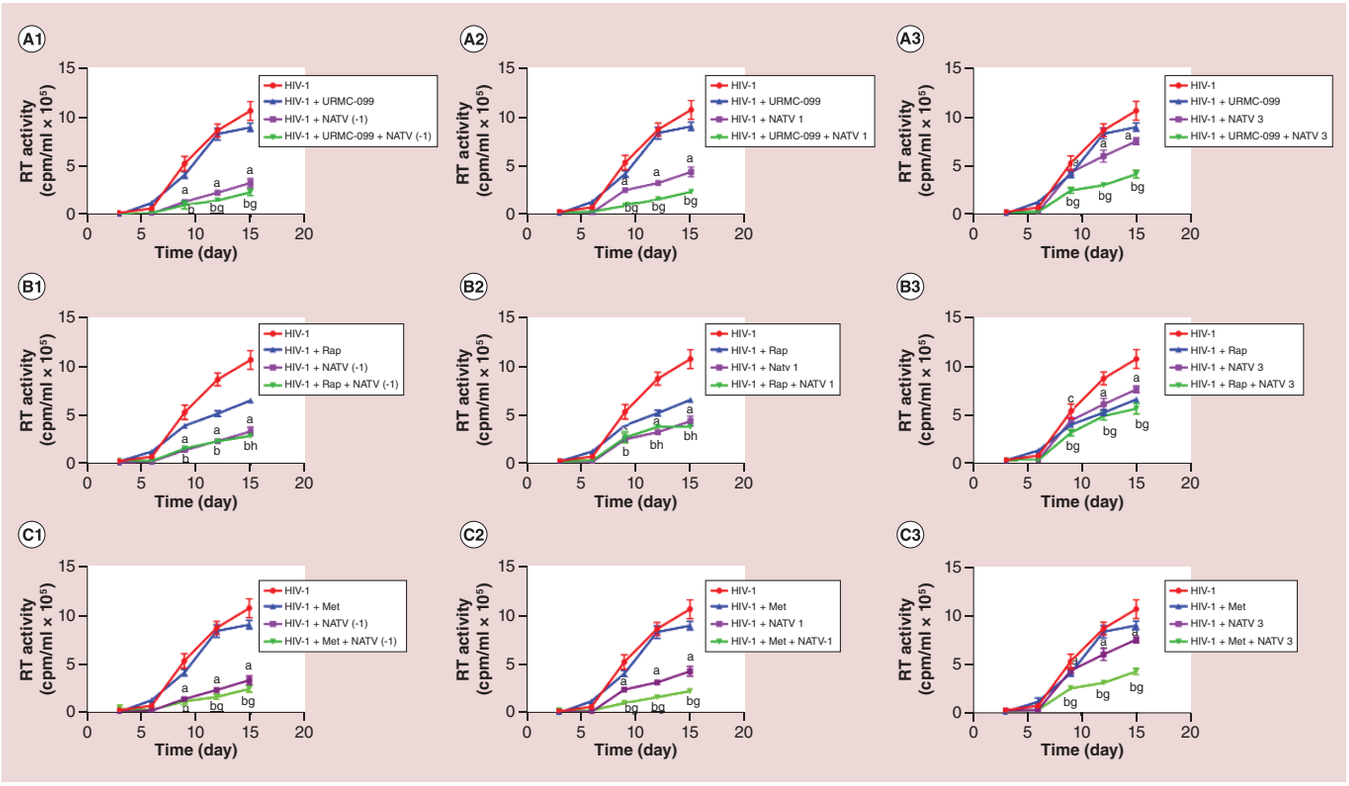

Figure 6. Effect of autophagy inducers on atazanavir antiretroviral activities. Human MDM were infected with HIV-1_{ADA} at an MOI of 0.1 then treated with 1 μM nanoATV on 1 day before **(A1–F1)** and 1 **(A2–F2)** and 3 days **(A3–F3)** after infection. Culture supernatant fluids were collected sequentially after infection and HIV-1 RT activity was measured. Data are represented as mean ± SD for n = 8 samples per group. Means compared by two-way ANOVA showing effect of treatment by time $p < 0.0001$. Pairwise comparison were performed with Bonferroni *post hoc* tests for $p < 0.05$. [a]$p < 0.0001$, [c]$p < 0.001$ and [e]$p < 0.01$ (HIV-1 infected controls compared with nanoATV). [b]$p < 0.0001$, [d]$p < 0.001$ and [f]$p < 0.01$ (HIV-1 infected controls compared with nanoATV and autophagy inducers). [g]$p < 0.0001$, [h]$p < 0.001$ and [i]$p < 0.01$ (nanoATV compared with nanoATV and autophagy inducers).
ATV: Atazanavir; MDM: Monocyte-derived macrophage; MOI: Multiplicity of infection; RT: Reverse transcriptase.

release. We posit that with further development of long acting autophagy agents, they as a group, could be used to influence drug delivery into viral reservoirs such as lymphoid tissues and gut leading to improved protection against infections and during treatment of chronic infections affect restorations of $CD4^+$ T effector memory cells [11,22]. In the context that these drugs were used in the current report harnessing autophagy not only led to prolonged

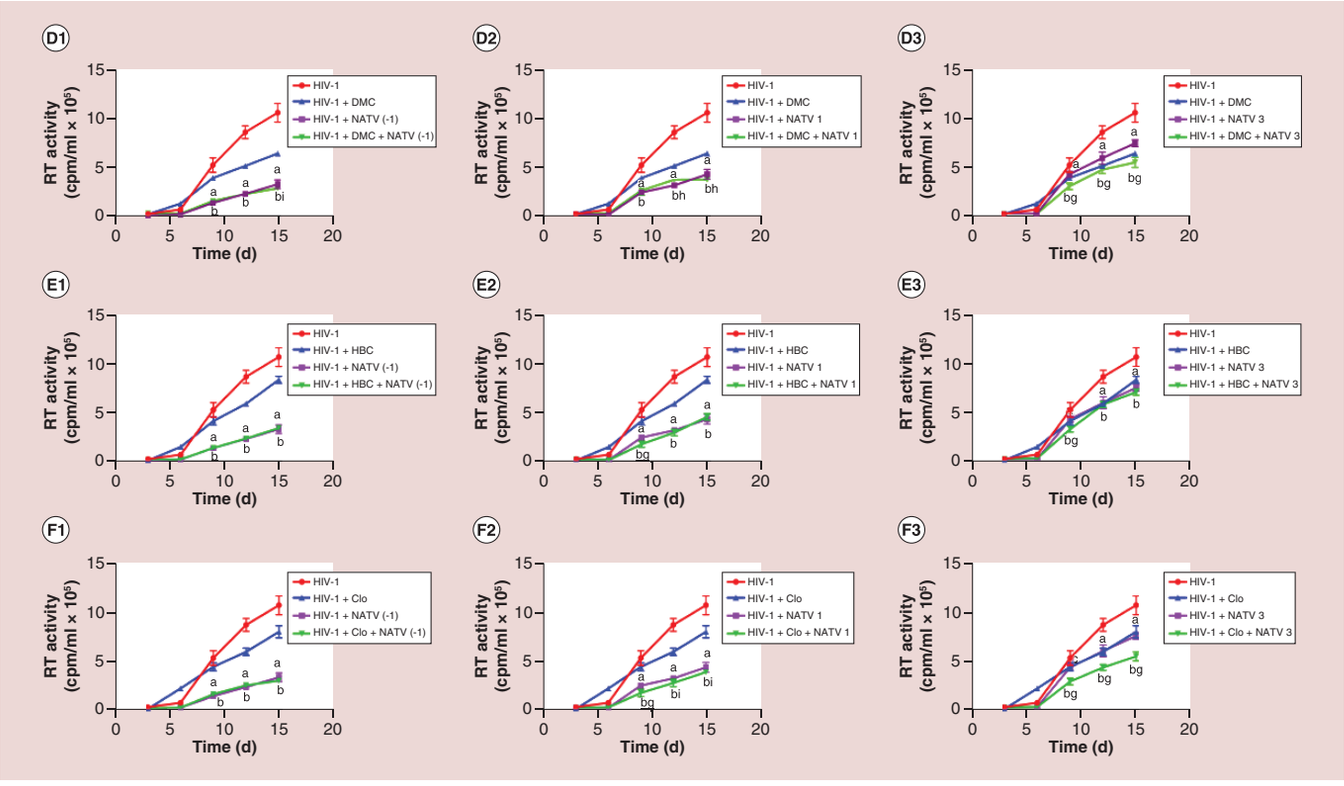

Figure 6. Effect of autophagy inducers on atazanavir antiretroviral activities (cont.). Human MDM were infected with HIV-1_{ADA} at an MOI of 0.1 then treated with 1 μM nanoATV on 1 day before **(A1–F1)** and 1 **(A2–F2)** and 3 days **(A3–F3)** after infection. Culture supernatant fluids were collected sequentially after infection and HIV-1 RT activity was measured. Data are represented as mean ± SD for n = 8 samples per group. Means compared by two-way ANOVA showing effect of treatment by time $p < 0.0001$. Pairwise comparison were performed with Bonferroni *post hoc* tests for $p < 0.05$. $^{a}p < 0.0001$, $^{c}p < 0.001$ and $^{e}p < 0.01$ (HIV-1 infected controls compared with nanoATV). $^{b}p < 0.0001$, $^{d}p < 0.001$ and $^{f}p < 0.01$ (HIV-1 infected controls compared with nanoATV and autophagy inducers). $^{g}p < 0.0001$, $^{h}p < 0.001$ and $^{i}p < 0.01$ (nanoATV compared with nanoATV and autophagy inducers).
ATV: Atazanavir; MDM: Monocyte-derived macrophage; MOI: Multiplicity of infection; RT: Reverse transcriptase.

drug half-life but accomplished the task by affecting drug depots and by positively affecting cell vitality. The latter was accomplished by enhancing the cells' mitochondrial activities and was found, at varying levels, for most of the autophagy agents tested.

Autophagy can affect the cellular reaction to injury and has been demonstrated to play important roles in cancer, degenerative diseases and HIV-1infection and its associated disorders [41–44]. Specific examples have been published by others. Rapamycin, notably, is a well-known inducer of autophagy and was shown to be effective, in part, in the treatment of cancers and in Huntington's and Alzheimer's diseases [45–48]. The mechanisms are related to mTOR-ULK1 inhibition coming active following the formation of a FKB12 cell complex then binding to mTORC1 and inhibition kinase activities [49]. Rapamycin can potentiate cell destruction when used in cancer chemotherapies [50]. URMC-099, in contrast, improves mitochondrial activities which increases the cell vitality [35,51,52].

Autophagosome formation was increased by all the autophagy inducing agents and was confirmed by studies of both BECN1 and LC3B I/II markers [53,54]. Each of the autophagy agents tested showed linkages to known published autophagy pathways and confirming their subcellular actions. In the current report, autophagosome formation and particle sequestration was confirmed by confocal microscopy after LC3B cell transfection. The tested autophagy inducers resulted in increased LC3B expression and autophagosome formation. Degradation of p62, a marker of autophagosome sequestration and one that determines autophagosome–lysosomal fusion is known to be operative during the completion of autophagy [55]. Higher levels of p62 indicates that slowing of autophagy flux and formation of autolysosomes by autophagosome lysosome fusion events is a likely mechanism for the retention of nanoARVs in autophagosomes [56,57]. ATV retention studies' results demonstrated that HBC, URMC-099 and clonidine promoted the maximum nanoATV retention as compared with the other inducers (Figure 3D).

Clonidine is known to induce autophagy through activation of Gi signaling pathways and does so in a mTOR independent manner. Activation of the Gi pathway results in the reduction of cAMP levels caused by the inhibition of adenylyl cyclase [58,59]. DMC is extensively used for psychiatric disorders and induces autophagy by blocking the degradation of the autophagic cargo [60]. Although DMC decreases autophagy flux and increases drug retention, it was the least effective for nanoATV retention, signaling that other operative mechanisms are present that extend drug depot formation. Nonetheless, using confocal imaging of drug particles colocalised with autophagosomes, autophagy inducers were demonstrated to help retain nanoATV in autophagosomes with URMC-099 being the most effective. In conclusion, although all autophagy inducers enhance the formation of autophagosomes, the flux of autophagosomal degradation varied between different autophagy inducers which had significant control in the cellular retention of drug depots. We do not know whether the differences in the kinetics of endosomal and autophagosomal degradation pathways also played a role in the higher retention of the drugs when autophagosomes were induced.

When HIV-1 infected macrophages were treated with nanoATV at 3 days after infection, all the autophagy inducing agents tested, except HBC, enhanced antiretroviral activities over drug nanoparticles alone. Though HBC showed a significant increase in nanoATV retention and autophagosome formation in MDM up to 14 days after treatment, the effect did not translate to inhibition of HIV-1 replication. HBC is approved by the US FDA as a drug delivery carrier to enhance stability and bioavailability of active agents. Unlike the other autophagy inducers, TFEB regulates autophagy and lysosomal biogenesis with HBC, and it is used in the treatment of Niemann–Pick disease, a cholesterol storage disorder [61]. Maximum improvement of the antiretroviral efficacy of nanoATV was achieved by URMC-099 out of all autophagy inducers tested.

HIV-1 and other viruses exploit host cell machinery for replication, dissemination and survival [62]. HIV-1 uses autophagosomes for their growth and maturation, where chronic HIV-1 infection inhibits cellular autophagy, an innate antiviral defence mechanism to avoid lysosomal degradation. HIV-1 infection in macrophages inhibits autophagy by Nef-mediated sequestration of TFEB in the cytoplasm [63]. URMC-099 assisted nuclear translocation of TFEB and thus overcomes HIV-1 Nef-mediated inhibition of autophagy [35]. Several autophagy inducers including rapamycin have been shown to inhibit HIV-1 infection by enhancing autophagosome and lysosome fusion, which ultimately inhibit HIV-1 infection [64–66]. This is clearly seen with rapamycin, clonidine and HBC, and a more significant inhibition is observed with DMC which coincides with lower LC3BII/I ratio suggesting increased autophagosome–lysosome fusion. The differences in the antiretroviral activity with some autophagy inducers is clear because of the increased autophagosome–lysosome fusion and increased autophagy flux with these inducers. The strong antiretroviral activities of these autophagy inducers suggest their potential as alternative therapeutics and adjunctive therapies for drug-resistant viral strains [41]. URMC-099 by itself consistently showed very little effect on viral replication, which might be because of reduced autophagosome degradation [11,35]. However, in the presence of nanoART, URMC-099 showed the highest antiretroviral activity which may be because of the higher retention of drugs in the autophagosomes or extended drug release. This needs further investigation.

Although ART has improved life expectancy and quality and decreased the prevalence of the most severe form of virus-associated dementia, it requires a life-long treatment regimen where adherence is often challenging [67]. Harnessing autophagy is a promising means to extend antiretroviral treatment duration. Thus, development of a long acting URMC-099 formulation could be employed as an adjunctive therapy to improve ARV treatment outcomes and bolster the use of long acting ART in disease preventative and treatment strategies.

Conclusion

In the present study, we have shown that autophagy inducers in general have the potential to facilitate sustained release of nanoATV. Comparative analysis of the different autophagy inducers proved that URMC-099 was the best among the lot. The sustained release is due to the formation of autophagosomes that enabled the intracellular retention of nanoATV. All of the parameters tested validated the ability of URMC-099 to affect ART effectiveness in restricting HIV-1 replication. This essentially emphasises that further research is warranted for URMC-099 as it could significantly improve the therapeutic efficiency of HIV-1 treatment regimens.

Future perspective

NanoART proved to be effective in antiretroviral treatment based on its long action, stability and slow drug release, in experimental conditions. The advantage of such formulations are the reduction in the therapeutic dosage of the drug used along with limited recorded side effects. Since treatment with a single drug alone is not able to suppress

viral replication without causing consequent viral mutations, the preferred strategy is combination therapy. This has proved to be effective but has led to recorded adverse effects. We show now that a spectrum of autophagy inducers could enhance the therapeutic potency of ARVs. We believe that the development of such agents could reduce the dosage frequency of ARVs and as such facilitate sustained release. Finding the 'best' autophagy inducer could ease combination ART and lead to sustained therapeutic benefits in preventing infection or viral transmission or by treating an already infected human host.

Summary points

- Present antiretroviral therapy requires increased dosage and frequency of administration to ensure that the drug concentration is maintained within the therapeutic window.
- Sustained release long acting nanoART can increase disage frequency and reduce drug toxicities.
- Autophagy can prolong cytoplasmic drug cargos.
- Upregulation of autophagy markers indicative of autophagosome formation was confirmed by Western blot analysis.
- Significant nanoformulated atazanavir intracellular retention was observed by 2-hydroxy-β-cyclodextrin, URMC-O99 and clonidine.
- URMC-099 and 2-hydroxy-β-cyclodextrin facilitated CF633 ATV-LC3B GFP colocalization.
- URMC-099 enhanced nanoformulated atazanavir antiretroviral activities.
- URMC-099 was the most effectivein enhancing antiretroviral activities.

Author's contributions

MB Thomas prepared the work plan, contributed to the data acquisition, analysis and interpretation of experimental results and wrote the manuscript. DP Gnanadhas codrafted the work plan and contributed to the analysis and interpretation of experimental results. PK Dash codeveloped the work plan and played a principal role in the manuscript preparation. J Machhi assisted in each of the western blot experiments and data analysis. Z Lin prepared and characterized the CF633-ATV and CF633-RPV nanoparticles. J McMillan guided in the handling of the UPLC instrument which was used for retention studies. B Edagwa developed the nanoparticles and provided valuable inputs towards the preparation of the manuscript. HA Gelbard provided insights on testing URMC-099 actions. S Gorantla and HE Gendelman designed the experiments, wrote the manuscript and contributed to the analysis and interpretation of experimental results. They critically read the edits provided by each of the authors and approved the final version.

Acknowledgements

The authors would like to thank B Kevadiya and A Bade and E Makarov and B Sillman for their technical assistance. The authors also appreciate the excellent technical assistantance provided by JA Taylor of the Advanced Microscopy Core Facility and members of the elutriation laboratory for their experimental support. DP Gnanadhas is presently a DST-INSPIRE faculty and affiliated to Centre for Nanotechnology and Advanced Biomaterials (CeNTAB), SASTRA, Thanjavur, Tamil Nadu, India.

Financial & competing interests disclosure

This work was supported, in part, by the University of Nebraska Foundation, which includes individual donations from C Swarts, H Singer and Frances and L Blumkin, and NIH grants P01 MH64570, RO1 MH104147, P01 DA028555, R01 NS36126, P01 NS31492, 2R01 NS034239, P01 NS43985, P30 MH062261 and R01 AG043540. URMC-099 is owned by URMC (HA Gelbard. lead inventor: patent nos. US 8,846,909 B2; 8,877,772; and 9,181,247 and associated international patents). No writing assistance was utilized in the production of this manuscript.

References

Papers of special note have been highlighted as: • of interest; •• of considerable interest

1. Richman DD, Margolis DM, Delaney M, Greene WC, Hazuda D, Pomerantz RJ. The challenge of finding a cure for HIV infection. *Science* 323(5919), 1304–1307 (2009).
2. Marsden MD, Zack JA. Eradication of HIV: current challenges and new directions. *J. Antimicrob. Chemother.* 63(1), 7–10 (2009).
3. Das MK, Sarma A, Chakraborty T. Nano-ART and NeuroAIDS. *Drug Deliv. Transl. Res.* 6(5), 452–472 (2016).
4. Kimata JT, Rice AP, Wang J. Challenges and strategies for the eradication of the HIV reservoir. *Curr. Opin. Immunol.* 42, 65–70 (2016).

5. Nowacek A, Gendelman HE. NanoART, neuroAIDS and CNS drug delivery. *Nanomedicine* 4(5), 557–574 (2009).
6. Nowacek A, Kosloski LM, Gendelman HE. Neurodegenerative disorders and nanoformulated drug development. *Nanomedicine* 4(5), 541–555 (2009).
7. Arainga M, Guo D, Wiederin J, Ciborowski P, Mcmillan J, Gendelman HE. Opposing regulation of endolysosomal pathways by long-acting nanoformulated antiretroviral therapy and HIV-1 in human macrophages. *Retrovirology* 12, 5 (2015).

• **Antiretroviral nanoparticles modulate the endolysosomal pathways.**

8. Dash PK, Gendelman HE, Roy U *et al.* Long-acting nanoformulated antiretroviral therapy elicits potent antiretroviral and neuroprotective responses in HIV-1-infected humanized mice. *AIDS* 26(17), 2135–2144 (2012).

• **Nanoformulated atazanavir improves the biodistribution and limits systmeic toxicities through systemic and targeted delivery.**

9. Guo D, Zhang G, Wysocki TA *et al.* Endosomal trafficking of nanoformulated antiretroviral therapy facilitates drug particle carriage and HIV clearance. *J. Virol.* 88(17), 9504–9513 (2014).
10. Martinez-Skinner AL, Arainga MA, Puligujja P *et al.* Cellular responses and tissue depots for nanoformulated antiretroviral therapy. *PLoS ONE* 10(12), e0145966 (2015).
11. Zhang G, Guo D, Dash PK *et al.* The mixed lineage kinase-3 inhibitor URMC-099 improves therapeutic outcomes for long-acting antiretroviral therapy. *Nanomedicine* 12(1), 109–122 (2016).

•• **URMC-O99 given in combination with nanoformulated atazanavir enhanced the antiviral responses.**

12. Li T, Gendelman HE, Zhang G *et al.* Magnetic resonance imaging of folic acid-coated magnetite nanoparticles reflects tissue biodistribution of long-acting antiretroviral therapy. *Int. J. Nanomed.* 10, 3779–3790 (2015).
13. Puligujja P, Arainga M, Dash P *et al.* Pharmacodynamics of folic acid receptor targeted antiretroviral nanotherapy in HIV-1-infected humanized mice. *Antiviral Res.* 120, 85–88 (2015).
14. Puligujja P, Balkundi SS, Kendrick LM *et al.* Pharmacodynamics of long-acting folic acid-receptor targeted ritonavir-boosted atazanavir nanoformulations. *Biomaterials* 41, 141–150 (2015).
15. Balkundi S, Nowacek AS, Veerubhotla RS *et al.* Comparative manufacture and cell-based delivery of antiretroviral nanoformulations. *Int. J. Nanomed.* 6, 3393–3404 (2011).
16. Roy U, Mcmillan J, Alnouti Y *et al.* Pharmacodynamic and antiretroviral activities of combination nanoformulated antiretrovirals in HIV-1-infected human peripheral blood lymphocyte-reconstituted mice. *J. Infect. Dis.* 206(10), 1577–1588 (2012).
17. Nowacek AS, Mcmillan J, Miller R, Anderson A, Rabinow B, Gendelman HE. Nanoformulated antiretroviral drug combinations extend drug release and antiretroviral responses in HIV-1-infected macrophages: implications for neuroAIDS therapeutics. *J. Neuroimmune Pharmacol.* 5(4), 592–601 (2010).
18. Edagwa BJ, Zhou T, Mcmillan JM, Liu XM, Gendelman HE. Development of HIV reservoir targeted long acting nanoformulated antiretroviral therapies. *Curr. Med. Chem.* 21(36), 4186–4198 (2014).
19. Arainga M, Edagwa B, Mosley RL, Poluektova LY, Gorantla S, Gendelman HE. A mature macrophage is a principal HIV-1 cellular reservoir in humanized mice after treatment with long acting antiretroviral therapy. *Retrovirology* 14(1), 17 (2017).
20. Guo D, Zhou T, Arainga M *et al.* Creation of a long-acting nanoformulated 2′,3′-dideoxy-3′-thiacytidine. *J. Acquir. Immune Defic. Syndr.* 74(3), e75–e83 (2017).
21. Zhou T, Su H, Dash P *et al.* Creation of a nanoformulated cabotegravir prodrug with improved antiretroviral profiles. *Biomaterials* 151, 53–65 (2018).
22. Cha W, Fan R, Miao Y *et al.* Mesoporous silica nanoparticles as carriers for intracellular delivery of nucleic acids and subsequent therapeutic applications. *Molecules* 22(5), 792–800 (2017).
23. Deodhar GV, Adams ML, Trewyn BG. Controlled release and intracellular protein delivery from mesoporous silica nanoparticles. *Biotechnol. J.* 12(1), 1600408 (2017).
24. Baert L, Van 'T Klooster G, Dries W *et al.* Development of a long-acting injectable formulation with nanoparticles of rilpivirine (TMC278) for HIV treatment. *Eur. J. Pharm. Biopharm.* 72(3), 502–508 (2009).
25. Dou H, Destache CJ, Morehead JR *et al.* Development of a macrophage-based nanoparticle platform for antiretroviral drug delivery. *Blood* 108(8), 2827–2835 (2006).
26. Garg M, Asthana A, Agashe HB, Agrawal GP, Jain NK. Stavudine-loaded mannosylated liposomes: *in vitro* anti-HIV-I activity, tissue distribution and pharmacokinetics. *J. Pharm. Pharmacol.* 58(5), 605–616 (2006).
27. Dutta T, Agashe HB, Garg M, Balakrishnan P, Kabra M, Jain NK. Poly (propyleneimine) dendrimer based nanocontainers for targeting of efavirenz to human monocytes/macrophages *in vitro*. *J. Drug. Target.* 15(1), 89–98 (2007).
28. Wan L, Zhang X, Pooyan S *et al.* Optimizing size and copy number for PEG-fMLF (N-formyl-methionyl-leucyl-phenylalanine) nanocarrier uptake by macrophages. *Bioconjugate Chem.* 19(1), 28–38 (2008).
29. Puligujja P, Mcmillan J, Kendrick L *et al.* Macrophage folate receptor-targeted antiretroviral therapy facilitates drug entry, retention, antiretroviral activities and biodistribution for reduction of human immunodeficiency virus infections. *Nanomedicine* 9(8), 1263–1273 (2013).

30. Nowacek A, Kadiu I, Mcmillan J, Gendelman HE. Immunoisolation of nanoparticles containing endocytic vesicles for drug quantitation. *Methods Mol. Biol.* 991, 41–46 (2013).

31. Kadiu I, Nowacek A, Mcmillan J, Gendelman HE. Macrophage endocytic trafficking of antiretroviral nanoparticles. *Nanomedicine* 6(6), 975–994 (2011).

32. Gendelman HE, Orenstein JM, Martin MA *et al.* Efficient isolation and propagation of human immunodeficiency virus on recombinant colony-stimulating factor 1-treated monocytes. *J. Exp. Med.* 167(4), 1428–1441 (1988).

33. Dey S, Subhasis Patro S, Suresh Babu N, Murthy PN, Panda SK. Development and validation of a stability-indicating RP–HPLC method for estimation of atazanavir sulfate in bulk. *J. Pharm. Anal.* 7(2), 134–140 (2017).

34. Kalter DC, Nakamura M, Turpin JA *et al.* Enhanced HIV replication in macrophage colony-stimulating factor-treated monocytes. *J. Immunol.* 146(1), 298–306 (1991).

35. Gnanadhas DP, Dash PK, Sillman B *et al.* Autophagy facilitates macrophage depots of sustained-release nanoformulated antiretroviral drugs. *J. Clin. Invest.* 127(3), 857–873 (2017).

•• **URMC-O99 facilitates sequestration of antiretroviral drugs and causes slow effective release of drug.**

36. Boska M, Liu Y, Uberti M *et al.* Registered bioimaging of nanomaterials for diagnostic and therapeutic monitoring. *J. Vis. Exp.* (46), e2459 (2010).

37. Kadiu I, Gendelman HE. Human immunodeficiency virus Type 1 endocytic trafficking through macrophage bridging conduits facilitates spread of infection. *J. Neuroimmune Pharmacol.* 6(4), 658–675 (2011).

38. Nowacek AS, Miller RL, Mcmillan J *et al.* NanoART synthesis, characterization, uptake, release and toxicology for human monocyte-macrophage drug delivery. *Nanomedicine* 4(8), 903–917 (2009).

39. Kadiu I, Gendelman HE. Macrophage bridging conduit trafficking of HIV-1 through the endoplasmic reticulum and Golgi network. *J. Proteome. Res.* 10(7), 3225–3238 (2011).

40. Zhang Z, Miah M, Culbreth M, Aschner M. Autophagy in neurodegenerative diseases and metal neurotoxicity. *Neurochem. Res.* 41(1–2), 409–422 (2016).

41. Levine B, Packer M, Codogno P. Development of autophagy inducers in clinical medicine. *J. Clin. Invest.* 125(1), 14–24 (2015).

• **Benefits and approaches employed for the development of autophagy inducers.**

42. Giordano S, Darley-Usmar V, Zhang J. Autophagy as an essential cellular antioxidant pathway in neurodegenerative disease. *Redox Biol.* 2, 82–90 (2014).

43. Harris H, Rubinsztein DC. Control of autophagy as a therapy for neurodegenerative disease. *Nat. Rev. Neurol.* 8(2), 108–117 (2011).

44. Nah J, Yuan J, Jung YK. Autophagy in neurodegenerative diseases: from mechanism to therapeutic approach. *Mol. Cells* 38(5), 381–389 (2015).

• **Modulation of stages of autophagy as a therapeutic strategy.**

45. Zhang L, Wang L, Wang R *et al.* Evaluating the effectiveness of GTM-1, rapamycin, and carbamazepine on autophagy and alzheimer disease. *Med. Sci. Monit.* 23, 801–808 (2017).

46. Li W, Gorantla S, Gendelman HE, Poluektova LY. Systemic HIV-1 infection produces a unique glial footprint in humanized mouse brains. *Dis. Model. Mech.* 10(12), 1489–1502 (2017).

47. Ricoult SJ, Manning BD. The multifaceted role of mTORC1 in the control of lipid metabolism. *EMBO Rep.* 14(3), 242–251 (2013).

48. Paquette M, El-Houjeiri L, Pause A. mTOR pathways in cancer and autophagy. *Cancers* 10(1), 10010018 (2018).

49. Takeuchi H, Kondo Y, Fujiwara K *et al.* Synergistic augmentation of rapamycin-induced autophagy in malignant glioma cells by phosphatidylinositol 3-kinase/protein kinase B inhibitors. *Cancer Res.* 65(8), 3336–3346 (2005).

50. Cheng PH, Lian S, Zhao R, Rao XM, Mcmasters KM, Zhou HS. Combination of autophagy inducer rapamycin and oncolytic adenovirus improves antitumor effect in cancer cells. *Virol. J.* 10, 293 (2013).

51. Kapuy O, Vinod PK, Banhegyi G. mTOR inhibition increases cell viability via autophagy induction during endoplasmic reticulum stress - an experimental and modeling study. *FEBS Open Bio.* 4, 704–713 (2014).

52. Lee J, Giordano S, Zhang J. Autophagy, mitochondria and oxidative stress: cross-talk and redox signalling. *Biochem. J.* 441(2), 523–540 (2012).

53. Pugsley HR. Assessing autophagic flux by measuring LC3, p62, and LAMP1 co-localization using multispectral imaging flow cytometry. *J. Vis. Exp.* (125), doi:10.3791/55637 (2017).

• **Understanding autophagic flux through the colocalization of autophagy markers.**

54. Pugsley HR. Quantifying autophagy: measuring LC3 puncta and autolysosome formation in cells using multispectral imaging flow cytometry. *Methods* 112, 147–156 (2017).

• **Assessment of autophagy by lysosomal marker analyses.**

55. Klionsky DJ, Abdelmohsen K, Abe A *et al.* Guidelines for the use and interpretation of assays for monitoring autophagy (3rd edition). *Autophagy* 12(1), 1–222 (2016).

56. Benjamin D, Colombi M, Moroni C, Hall MN. Rapamycin passes the torch: a new generation of mTOR inhibitors. *Nat. Rev. Drug Discov.* 10(11), 868–880 (2011).
57. Cao C, Subhawong T, Albert JM *et al.* Inhibition of mammalian target of rapamycin or apoptotic pathway induces autophagy and radiosensitizes PTEN null prostate cancer cells. *Cancer Res.* 66(20), 10040–10047 (2006).
58. Chao HM, Osborne NN. Topically applied clonidine protects the rat retina from ischaemia/reperfusion by stimulating alpha(2)-adrenoceptors and not by an action on imidazoline receptors. *Brain Res.* 904(1), 126–136 (2001).
59. Osborne NN. Inhibition of cAMP production by alpha 2-adrenoceptor stimulation in rabbit retina. *Brain Res.* 553(1), 84–88 (1991).
60. Rossi M, Munarriz ER, Bartesaghi S *et al.* Desmethylclomipramine induces the accumulation of autophagy markers by blocking autophagic flux. *J. Cell Sci.* 122(Pt 18), 3330–3339 (2009).
61. Davidson CD, Ali NF, Micsenyi MC *et al.* Chronic cyclodextrin treatment of murine Niemann-Pick C disease ameliorates neuronal cholesterol and glycosphingolipid storage and disease progression. *PLoS ONE* 4(9), e6951 (2009).
62. Tang SW, Ducroux A, Jeang KT, Neuveut C. Impact of cellular autophagy on viruses: insights from hepatitis B virus and human retroviruses. *J. Biomed. Sci.* 19, 92 (2012).
63. Campbell GR, Rawat P, Bruckman RS, Spector SA. Human immunodeficiency virus type 1 nef inhibits autophagy through transcription factor EB sequestration. *PLoS Pathogens* 11(6), e1005018 (2015).
64. Roy J, Paquette JS, Fortin JF, Tremblay MJ. The immunosuppressant rapamycin represses human immunodeficiency virus type 1 replication. *Antimicrob. Agents Chemother.* 46(11), 3447–3455 (2002).
65. Donia M, Mccubrey JA, Bendtzen K, Nicoletti F. Potential use of rapamycin in HIV infection. *Br. J. Clin. Pharmacol.* 70(6), 784–793 (2010).
66. Sagnier S, Daussy CF, Borel S *et al.* Autophagy restricts HIV-1 infection by selectively degrading Tat in $CD4^+$ T lymphocytes. *J. Virol.* 89(1), 615–625 (2015).
67. Eggers C, Arendt G, Hahn K *et al.* HIV-1-associated neurocognitive disorder: epidemiology, pathogenesis, diagnosis, and treatment. *J. Neurol.* 264(8), 1715–1727 (2017).